J. Appl. Comput. Mech., 7(4) (2021) 1907–1915
DOI: 10.22055/JACM.2020.32902.2097

ISSN: 2383-4536
jacm.scu.ac.ir

Shahid Chamran University of Ahvaz

Journal of Applied and Computational Mechanics

Research Paper

Nanostructure, Molecular Dynamics Simulation and Mechanical Performance of PCL Membranes Reinforced with Antibacterial Nanoparticles

Ashkan Farazin[1], Farshid Aghadavoudi[1], Mehdi Motiifard[2], Saeed Saber-Samandari[3], Amirsalar Khandan[3]

[1] Department of Mechanical Engineering, Khomeinishahr Branch, Islamic Azad University, Khomeinishahr/Isfahan, Iran, Email: ashkanfarazin@gmail.com, davoodi@iaukhsh.ac.ir

[2] Department of Orthopedic Surgery, School of Medicine, Isfahan University of Medical Sciences, Isfahan, Iran, Email: Motiifard@med.mui.ac.ir

[3] New Technology Research Center, Amirkabir University of Technology, Tehran, Iran, Email: saeedss@aut.ac.ir, amir_salar_khandan@yahoo.com

Received March 10 2020; Revised March 27 2020; Accepted for publication March 27 2020.
Corresponding author: Amirsalar Khandan (amir_salar_khandan@yahoo.com)

Abstract: Recently, the application of porous bio-nanocomposites has been considered by many researchers for orthopedic application. Since experimental tests for obtaining the mechanical and physical properties of these nanostructured biomaterials are very expensive and time-consuming, it is highly recommended to model and simulate these bio-nanoscale materials to predict their mechanical and physical properties. In this study, three-phase porous bio-nanocomposite membranes were fabricated with Titanium oxide (TiO_2), Hydroxyapatite (HA) and Polycaprolactone (PCL) polymer. HA and TiO_2 are both biocompatible and biodegradable. The samples were fabricated with various amounts of titanium oxide and the materials characterization has been performed on selected sample. The molecular dynamics technique (MD) have been used to predict the mechanical performance of the nanocomposite models. The MD simulations were performed for single phase material and the developed for two phases equivalent components as a new approach in using MD simulation results. The results indicated the close relationship between the experimental data and simulation values for the selected sample. Moreover, phase and morphology of these nanostructures have been investigated using SEM results. Therefore, based on the proposed approach, MD simulation can be applicable for predicting the properties of porous bio-nanocomposite membrane.

Keywords: Molecular dynamics, Polycaprolactone, Hydroxyapatite, Mechanical performance, Nanocomposite membrane.

1. Introduction

During last two decades, many researchers have considered molecular dynamics (MDs) as a new technique for prediction and modelling of nano- microstructures materials. MD is utilized by many engineering majors such as biomedical, chemical, mechanical, and genetic to decrease experimental costs in the laboratory's evaluation [1-2]. Moreover, MD tools can be applied for new materials with new properties that are not recorded anywhere [3-4]. The MD softwares such as Materials Studio and LAMMPS can speed up the computation and calculation of the measurements and predicting the material properties in engineering and medicine [5-6]. Use of the classical theories such as micro-mechanics for analyzing and measuring the mechanical properties of nanocomposites is not a powerful technique. On the other hand, the precision and possibilities of MD technique is a matter of debate among all researchers [7-13]. The MD tools are known as an empirical-experimental technique to calculate the nanostructure properties in terms of chemical compositions and force field of atoms [14-18]. In the polymeric field bio-nanocomposites, polymer properties are strongly dependent on the structural complexity or morphology (nanostructured shape) of polymer molecules. In the MDs method, according to defined potential functions, the atomic microstructure of molecules can be simulated. Then, the equilibrium the obtained physical or mechanical results through statistical mechanics can be achieved [19-22].

In the field of MD, Aghadavoudi et al. [23] tested and investigated the effect of defected carbon nanotubes (CNTs) on the mechanical properties of nanocomposites with epoxy matrix using MD and evaluated the elastic modulus changes, Montazeri et al. [24] evaluated the effect of CNTs orientation on the shear deformation properties of composite polymers by the combination of MD and finite element analysis (FEA). Their results illustrated that in the 45° direction, single-walled carbon nanotubes (SWCNT) had the greatest effect on the shear modulus. Marcadon et al. [25] applied an MD approach to investigate the effect of nanoscale particles on the properties of polymer nanoparticles. In their research, MD simulation have been used for modeling of silica polymer based nanaocmposite. The results showed that the elastic modulus increases with particle size. An ideal porous scaffold with appropriate porosity and strength must be non-toxic, biocompatible, with good tensile and compressive mechanical strength.

Published online: April 08 2020

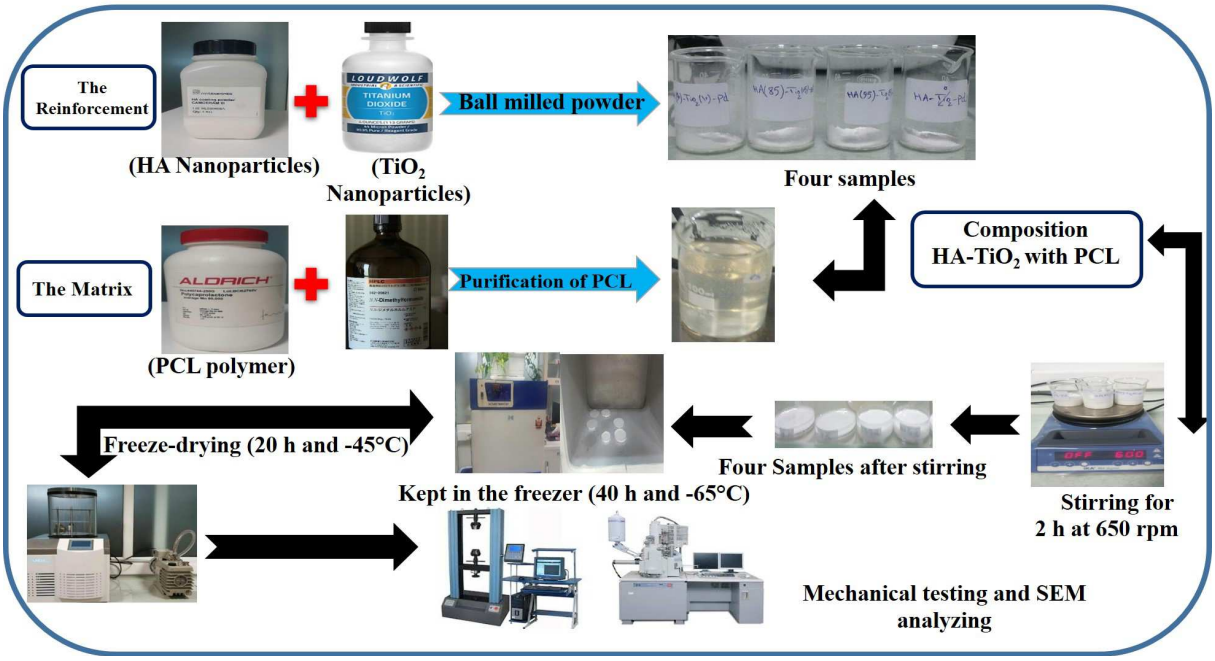

Fig. 1. Schematic of fabrication stages polymeric bio-nanocomposite reinforced with HA and TiO_2 nanoparticles

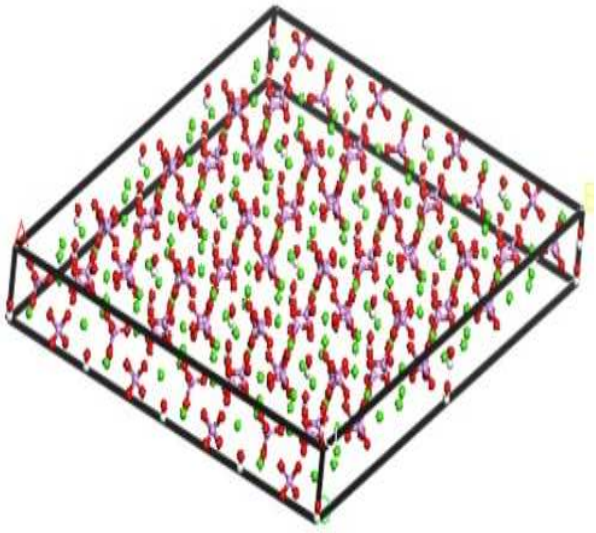

Fig. 2. Simulation box for modeling the hydroxyapatite

Also, it must have a neutral biological environment, capable of supporting cell adhesion, growth, and cell differentiation at the micrometer scale. It should contain a good degradation rate for reconstitution of the cells and its porosity size allows the cells to grow [16-23]. Farazin et al. [26] investigated the mechanical behavior of porous bio-nanocomposite such porosity and elastic modulus of the samples by micromechanical models using experimental results. Their results indicated some theories like Dewey's method have some error for the prediction of mechanical properties for porous nanocomposite. The novelty of the current work is predicting the mechanical properties of a porous bio-nanocomposites membrane based on MD simulation results. The MD simulations were performed on porous bio-nanocomposite models containing 0 wt%, 5 wt%, 10 wt%, and, 15 wt% titanium oxide. Experimental values and predicted results have been compared and slight differences were observed.

2. Materials and Methods

In the current work, molecular models of three-phase nanocomposite have been constructed based on empirical data. The fabrication stages of the nanocomposite using freeze drying technique is shown Fig. 1 and modeling details are in accordance with the results presented in the previous research [26]. The chemical formulas of nanocomposite constituents including (PCL-HA-TiO_2) are shown in Table 1.

After constructing the molecular structures on MD, amount of substance (N), volume (V) and temperature (T) and amount of substance (N), pressure (P) and temperature (T) as (NVT-NPT) conserved for evaluating the mechanical and physical properties. Computational MDs simulation can be used as a useful technique to predict the specific behavior of macromolecules under different conditions. Therefore, in a system with the assumption of intermolecular interactions one can accurately predict the properties of the mass in question. But one of the weaknesses of MDs is the inability of the material with transverse and longitudinal bonds and high temperature changes to predict [26]. In addition, one can prove the validity or incorrectness of a theory by comparing the results of a simulation and with experimental data.

Table 1. Chemical formula and pure materials for fabrication of porous bio-nanocomposites

Materials for fabrication bio-nanocomposite	Chemical formula
Hydroxyapatite	$Ca_5(PO_4)_3(OH)$
Titanium oxide	TiO_2
Polycaprolactone	$(C_6H_{10}O_2)_n$

Table 2. Comparison of mechanical and physical properties of HA, TiO_2 nanoparticles, and PCL polymer using molecular dynamics method and experimental results

Comparison of mechanical and physical properties of crystal HA using MD with experimental amounts		
Mechanical and physical properties	**Molecular dynamics simulation results**	**Experimental results**
Density (g/cm³)	4.15	3.21 [17]
Elastic modulus (MPa)	109.709	110 [17]
Poisson's ratio (--)	0.307	0.27 [17]
Comparison of mechanical and physical properties of TiO_2 using MD with experimental amounts		
Mechanical and physical properties	**Molecular dynamics simulation results**	**Experimental results**
Density (g/cm³)	3.94	4.2 [18]
Elastic modulus (MPa)	180.165	230 [18]
Poisson's ratio (--)	0.297	0.3 [18]
Comparison of mechanical and physical properties of PCL using MD with experimental amounts		
Mechanical and physical properties	**Molecular dynamics simulation results**	**Experimental results**
Density (g/cm³)	1	1.1 [19]
Elastic modulus (MPa)	3.3	1.2 [19]
Poisson's ratio (--)	0.36	0.3 [19]

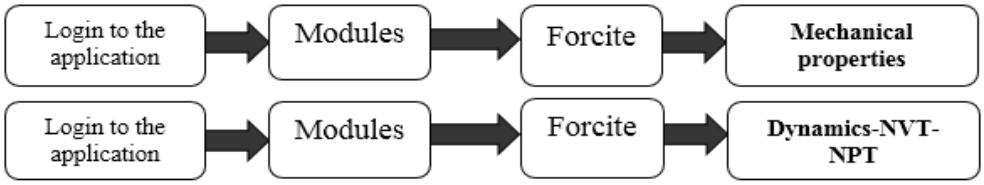

Fig. 3. Steps to obtain the mechanical and physical properties of two-phase molecular models using Materials Studio software

The nanostructure of the pure material is simulated separately, and then elastic behavior is investigated. Then, due to the MD constraints, at first two basic two-phase including a polymer and one reinforcement were simulated separately, and its mechanical properties were extracted by MD. Then, with the help of a proposed micro-mechanical relation, the mechanical properties of the three-phase membrane were extracted and compared with experimental results. In the recent years, the application of bioceramics, such as bioactive hydroxyapatite, has been increased for medical and dental applications [27-35]. The HA is very similar to bone and tooth of human with the chemical formula of ($Ca_{10}(PO_4)_6(OH)_2$) [36-42]. The simulation box for modeling the HA is shown in the Fig. 2 Titanium oxide nanoparticles with a chemical formula of (TiO_2) have been used as a reinforcement for the modeling of bio-nanocomposite due to the high elastic modulus of titanium oxide nanoparticle. The biocompatible properties of TiO_2 mineral oxide bone is today used as the main building for implants in dental science [33]. The PCL polymer is a hydrophobic semi-crystalline polymer with molecular formula $(C_6H_{10}O_2)$n. The PCL polymer has extraordinary properties such as proper mechanical flexibility, good biocompatibility, simple and easy processability, low melting point (T_m = 60°C) and biodegradable behavior.

2.1. Physical and mechanical simulation using MD

The physical and mechanical properties of the simulation boxes were extracted in MD software using the stages which are shown in Fig. 3. The following steps have been taken to implement the molecular dynamics method. At this stage, the simulation box is placed at a temperature of 300 K under NVT condition. The purpose of NVT is to increase the energy of the system in which atoms have the potential energy required to move towards balanced system. In other words, the reason for applying NVT is to eliminate the initial internal stress of molecular structure that was applied at the time of the construction of the simulation box. At this stage, the initial density of the system (0.9 g/cm³) is assumed. The simulation time is assumed 30 ps. Then, the initial pressure of system is at 1 atm with a temperature of 300 K under a constant NPT to close the system density to the actual density. NPT can also eliminate the system tensions.

3. Results and Discussion

The obtained results of the porous bio-nanocomposite molecular modeling presented in Fig. 4 and Fig. 5. The outcome results cover physical and mechanical properties including density, elastic modulus, and Poisson's ratio. The obtained results were compared with the experimental results to find the optimum values. It should be noted that in the first step, the results of the MDs of pure materials were checked and validated. Then, the results of the two-phase MDs of (HA-PCL) and (TiO_2-PCL) were investigated separately. Finally, a three-phase nanosized composite was analytically performed. In the first step, mechanical properties (elastic modulus and Poisson's ratio), and physical properties (density) of pure materials were obtained and validated by experimental tests. To obtain the density diagram, first, NVT for simulated nanocomposite model was used to maximize the system energy and then the NPT was applied to plot the density diagram. Table 2 shows the mechanical and physical properties of HA with TiO_2 nanoparticles and PCL compared with MD modeling observations.

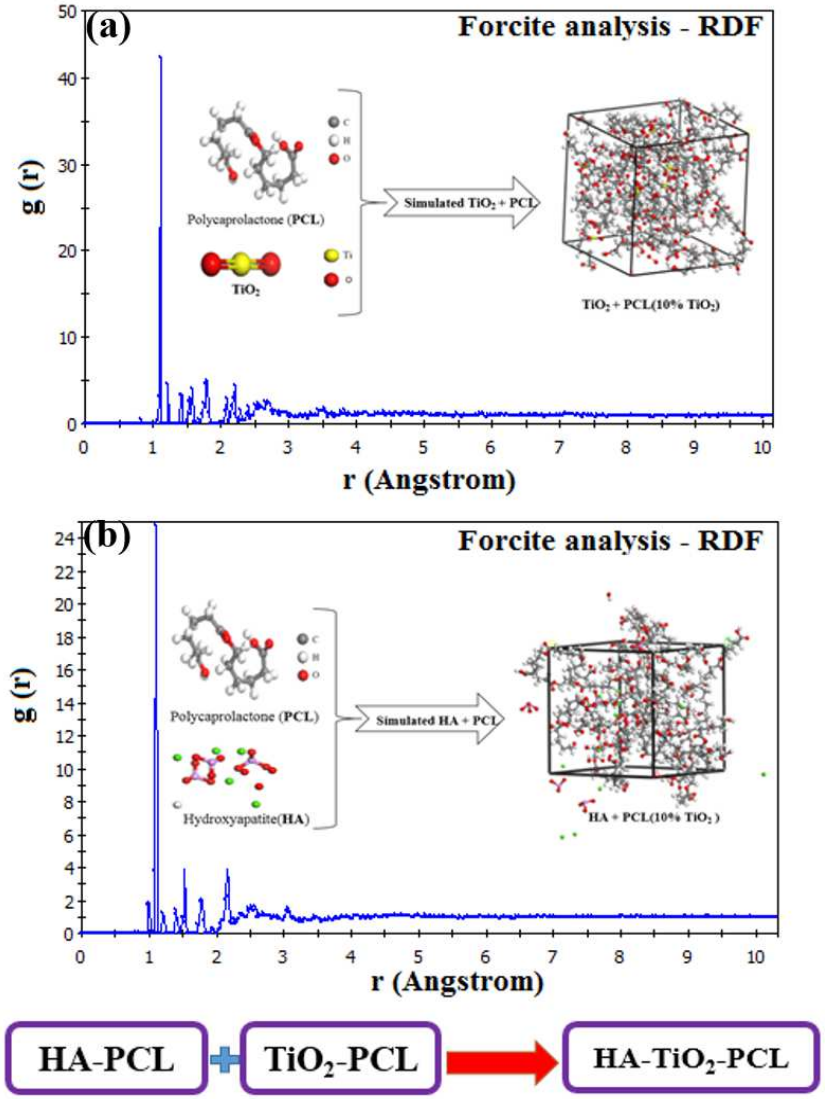

Fig. 4. RDF diagram of (a) TiO_2-PCl, and (b) HA-PCL nanocomposite with 10 wt% TiO_2

The mechanical properties (elastic modulus and Poisson's ratio) and the physical properties (density value) of two-phase nanocomposites including (HA-PCL and TiO_2-PCL) with various amount of 0, 5, 10 and, 15 wt% of TiO_2 were calculated individually. To reduce the number of graphs, the sample with 10 wt% of TiO_2 was selected and the obtained results were discussed for further investigations. In this section, HA nanoparticles with a specific weight percentage (16.66%) and PCL with a specific weight percentage (83.33%) was simulated in the Materials studio software. The RDF (Radial Distribution Function) diagram of the nanosized composite shown in Fig. 4 (a-b) for accuracy of the molecule's placement. In the RDF diagram, the necessary and sufficient convergence is the number 1. To illustrate the density diagram, NVT was used and then, the NPT was applied. The density diagrams of the simulated nanocomposite represented in Fig. 5(a-b), which show the density of the simulation boxes of nanocomposites have been converged to 1 g/cm^3.

For plotting the density diagram of two-phase (HA-PCL) nanocomposite, the temperature was assumed 300 K, and the simulation time was assumed 30 ps. After calculating the mechanical properties, elastic modulus was reported to be near 0.04 GPa and the Poisson's ratio was calculated approximately 0.3.

In this section, the TiO_2 reinforcement with a specific weight percentage (11.76%) and PCL with a specific weight percentage (88.23%) was simulated in the materials studio software. To draw the density diagram, a simulated NVT model was used, and then the NPT was applied to plot the density diagram. For plotting the density of two-phase (TiO_2-PCL) nanocomposite, the temperature was assumed 300 K, and the time was simulated in 30 ps. After calculating the mechanical properties, elastic modulus was reported to be approximately 0.02 GPa and the Poisson's ratio was set near 0.4.

Table 3 shows the results for the MD simulation of two-phase molecular models and their mechanical properties. The main propose of this article is to extract and simulate the physical and mechanical properties of three-phase nanocomposite by MD technique. Direct simulation of three-phase nanosized composites with MDs tools faced with computational constraints. In the molecular modeling, the placement of pure material atoms in the molecular structure of the three-phase nanocomposites should be carried out in such a way that the atomic distances in model are similar to the actual atomic intervals in microstructure that causes an over-dimensional increase in the simulation box. In fact, in order to create a similar real model it is necessary to create a simulation box with dimension about 100 nm or 1000 A° which is not possible now due to computational constraints. In this study, to create a comprehensive model, a combination of molecular structure and micromechanical methods is developed to derive the properties of the three-phase nanocomposite from the two-phase models. Finally, the properties of two-phase models (HA-PCL) and (TiO_2-PCL) were extracted using MD results.

Table 3. The results of simulation two-phase with molecular dynamics method and its experimental results mechanical properties

Sample	Combinations	Elastic Modulus (MPa)	Poisson's Ratio
HA+PCL	HA (16.66%)-PCL (83.33%)	1620	0.3
TiO_2+ PCL	TiO_2 (11.76%)-PCL (83.23%)	2080	0.4

Table 4. Mass and volume fraction in a three-phase simulated samples

Sample	Mass of matrix and reinforcements (gr)			Volume fraction (%)			No. of atoms	Lattice dimensions (A°)
	TiO_2	HA	PCL	TiO_2	HA	PCL		
0 wt% TiO_2	0	2	6	0	7.5	92.5	1561	20.3×20.3×20.3
5 wt% TiO_2	0.4	1.6	6	1.5	6	92.5	1563	20.5×20.5×20.5
10 wt%TiO_2	0.8	1.2	6	3	4.5	92.5	1572	20.8×20.8×20.8
15 wt%TiO_2	1.2	0.8	6	4.5	3	92.5	1674	21×21×21

Table 5. Volume fractions of two-phase equivalent model for three-phase bio- nanocomposite

sample (0 wt% TiO_2)			
HA	PCL	PCL	HA
3.75	46.25	46.25	3.75
sample (5 wt% TiO_2)			
HA	PCL	PCL	TiO_2
6	46.25	46.25	1.5
sample (10 wt% TiO_2)			
HA	PCL	PCL	TiO_2
4.5	46.25	46.25	3
sample (15 wt% TiO_2)			
HA	PCL	PCL	TiO_2
3	46.25	46.25	4.5

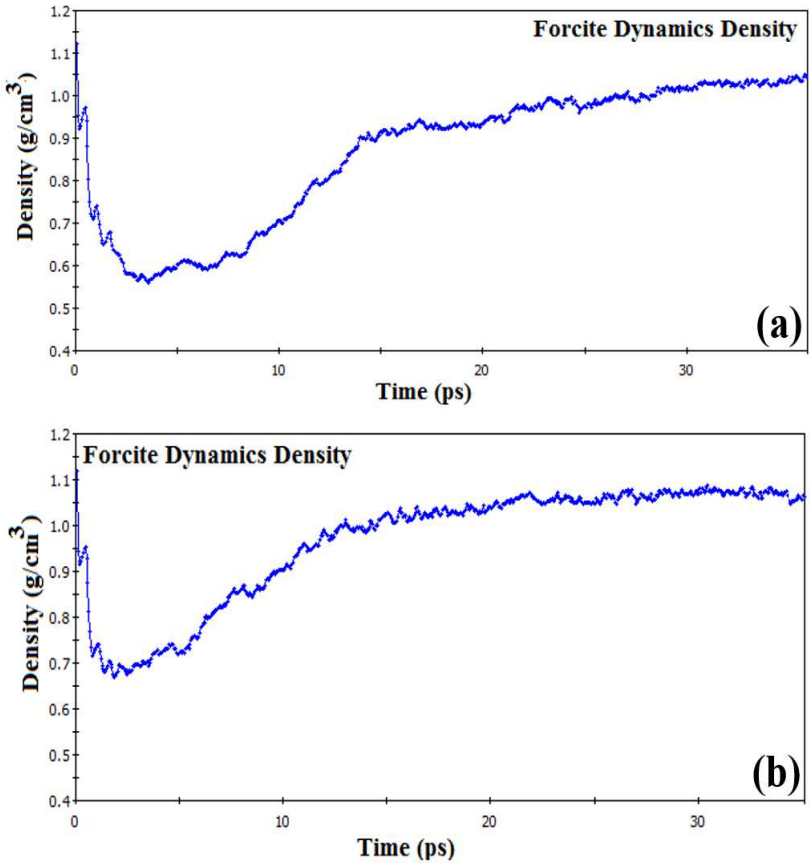

Fig. 5. Density diagram of two-phase simulated two-phase nanocomposite simulation box (a) HA-PCL, and (b) TiO_2-PCl nanocomposite with 10 wt% TiO_2

Then, the computation of volumetric and weight fraction for three-phase model components in terms of volume and weight fraction of two-phase models was performed. Then, the mechanical and physical properties of the three-phase were extracted by micromechanical relations. The mechanical and physical properties of two-phase molecular models were reported in the previous section. The rule of mixtures (ROM) relationships are used to convert the volumetric and weight fractions from two-phase to three-phase. Table 4 shows the volume fraction related to the elemental constituents of the nanocomposites. The values in the Table 4 are calculated based on the density of the constituents.

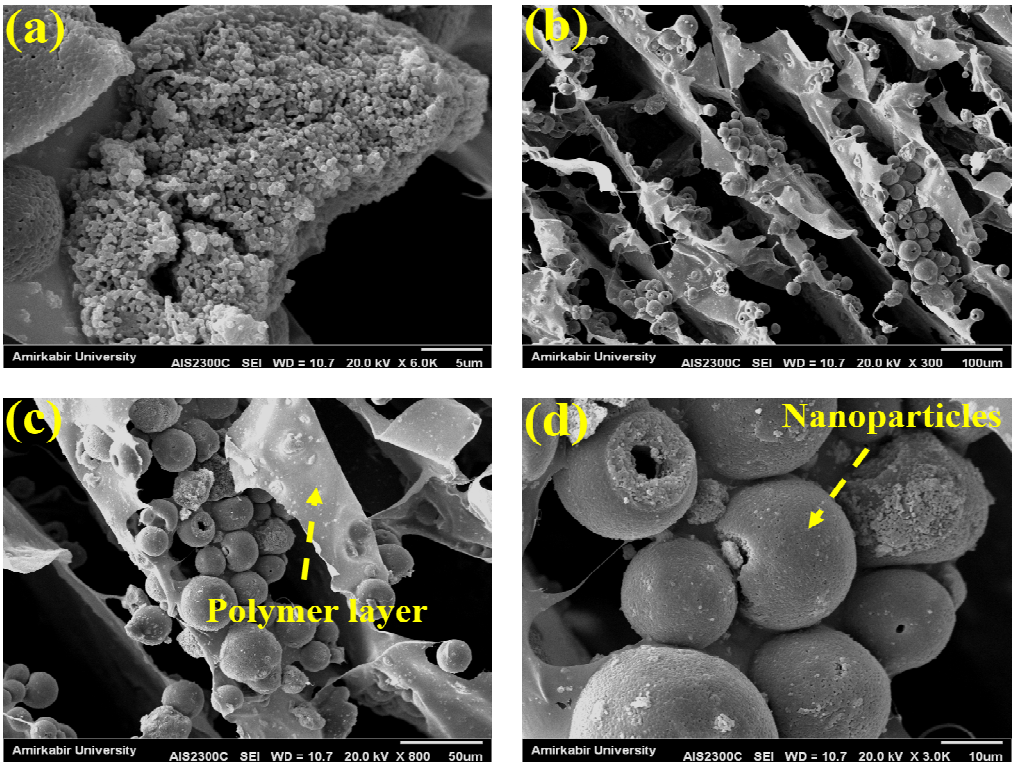

Fig. 6. SEM image of porous bio-nanocomposite scaffolds containing (a) 5 wt%, (b) 10 wt%, (c) 15 wt%, and (d) magnified 15 wt% of TiO_2

For the three-phase simulation, it is assumed that the three-phase composite is composed of two-phase material and accordingly, the volume fractions of the equivalent constituents in the two-phase material are calculated. The obtained values are shown in Table 5.

Given that the equivalent model is divided into two separate sections, the following general equation is suggested for calculating the elastic modulus of three-phase nanocomposite based on molecular modeling results as shown in following equation,

$$E = K(\alpha_i a V_{2P-HP} E_{2P-HP} + \beta_i b V_{2P-TP} E_{2P-TP}) \tag{1}$$

In the above equation, the parameters are defined as follows:

K : Structural porosity coefficient

α_i : The volume fraction correction factor of a two-phase molecular model (HA + PCL)

β_i : The volume fraction correction factor of a two-phase molecular model (TiO_2 + PCL)

a : Effective fiber coefficient for the two-phase (HA + PCL) sample

b : Effective fiber coefficient for the two-phase (TiO_2 + PCL) sample

V_{2P-HP} : Volume fraction of two-phase (HA + PCL) equivalent model in a three-phase sample

V_{2P-TP} : Volume fraction of two-phase (TiO_2 + PCL) equivalent model in a three-phase sample

E_{2P-HP} : Elastic modulus of two-phase (HA + PCL)

E_{2P-TP} : Elastic modulus of two-phase (TiO_2 + PCL)

By substituting the values of the mechanical properties of the Table 3 in Eq. 1, the predicted value for the elastic modulus is calculated, which is slightly different from the experimental value. For example, for sample 10% TiO_2 the calculated elastic modulus for the porous nanocomposite membrane is 60MPa which is about 10% more than experimental result (55 MPa).

In the current research, a case study performed on the (PCL-HA-TiO_2) porous bio-nanocomposite fabricated using freeze drying technique. Therefore, the SEM microphotographs and surface morphology of the samples were evaluated on porous bio-nanocomposite scaffolds. Figure 6 (a-d) shows the SEM images of the well porous scaffold with spherical shape on the PCL layer surrounded by TiO_2 nanoparticles. Figure 6 shows the pores are interconnected and can interact with each other to help internal communication in trapping the drug and nutrients. The walls of these porosities consist of PCL, HA, and TiO_2 nanoparticles have micron size less than 50 micron. The amount of HA nanoparticles directly affects the morphology of the scaffold. These porosities are in the same direction (closed holes are barely visible), suggesting that the microstructure implemented in bone tissue can have potential applications in orthopedic field [38-42]. Also, Figure 6 (a-d) shows the SEM images of the porous bio-nanocomposite with regular and non-regular cavities that simulated using the mechanical software and found that the flow of regular bio-nanocomposites is more than those with the same geometry. Therefore, it can be concluded that due to the regular distribution of drug and bioceramic reinforcement that enhance the mechanical properties of the scaffolds with cavities and the regular microstructure can heal the compounds. The SEM images have shown that the increase in cell proliferation rate affected by the association of the cells with the bioactive surface and the porosity of the antibacterial scaffold in the range of 10-30 microns. Also, intercellular communication with the presence of antibacterial nanoparticles in the hydroxyapatite bioactive ceramic improved, indicating activation of chemical and biological communication mechanisms between cells [35-39]. The SEM images also appears that polymeric scaffolds with larger cavity size increase the chances of adhesion of epithelial cells to the substrate and can therefore be used as a substrate made of natural materials for tissue engineering purposes.

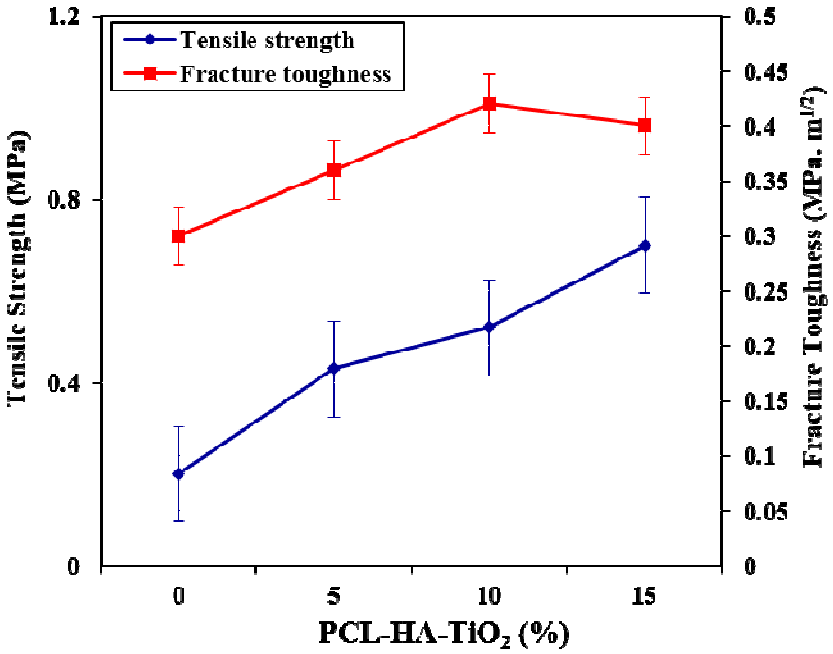

Fig. 7. Variation of Tensile strength and fracture toughness of bio-nanocomposites (PCL-HA-TiO_2) with percent of TiO_2

Therefore, SEM image shows the proper chemical stability of the architecture of porous tissue without degradation. One of the fundamental challenges in tissue engineering is the fabrication of three-dimensional scaffolds with high porosity and sufficient tensile strength, in case in this work addition of antibacterial nanoparticles increased the tensile more than three times. The increased of tensile strength and density of the porous material can be due to the addition of titanium nanoparticles. It was also shown that increasing the titanium content increases the ability of the apatite layer to form on the surface of the porous material. Using freeze drying technique has been used to fabricate PCL polymeric scaffolds, which has resulted in desirable mechanical properties. It is noteworthy that the microstructure of the 3D antibacterial nanoparticles can support, enhance cell adhesion and proliferation. The SEM images show the size of the pores at the micron scale, which is within the proper range of cell nucleation and growth. Polymer and antibacterial nanoparticles are nanostructured with large multilayered networks where culture conditions can alter the morphology of the layers. Figure 6 shows that the addition of TiO_2 nanoparticles increased the chemical stability of the samples. Also, the SEM image shows that chemical and physical adhesion between the polymeric substance and ceramic part successfully achieved in the sample containing 10 wt% TiO_2 compared to other scaffolds. Figure 7 shows that with increasing the TiO_2 weight percentage in a porous nanostructure, the tensile strength of the sample increased from 0.2 MPa to 0.7 MPa. The tensile strength results indicated that the spherical shape of TiO_2 increased the mechanical properties of the sample more than three times, in which the experimental observation approved the obtained results from the simulation. The fracture toughness values were determined by calculating the area under the stress-strain diagram and the elastic modulus value of the scaffold from the slope of the stress-strain curves.

Also, the average size of the cavities of this scaffold was calculated to be 20–50 micron, which is desirable for the growth and proliferation of the cells. By measuring the cavities, it was concluded that the presence of bioceramic phase increased the porosity in the porous bio-nanocomposite scaffolds.

4. Conclusion

Mechanical properties (Poisson's ratio and elastic modulus) of three-phase bio-nanocomposite were calculated using MD simulation results. The obtained results show that the proposed method for predicting the elastic modulus of nanocomposite membrane is accurate because the for different weight fraction of nanoparticles the differences between actual measurements and calculated values are negligible. Therefore, this method can be used to study the effect of physical parameters affecting on mechanical properties in three-phase nanocomposites. SEM microphotographs and surface morphology showed the average size of the cavities of this scaffold was calculated to be 20–50 micron, which is desirable for the growth and proliferation of the cells. It was also shown that increasing the titanium content increases the ability of the apatite layer to form on the surface of the porous material. Freeze drying technique has been used to fabricate PCL polymeric membrane, which has resulted in desirable mechanical properties.

Author Contributions

All authors contributed the same. The manuscript was written through the contribution of all authors. All authors discussed the results, reviewed, and approved the final version of the manuscript.

Acknowledgments

The authors would like to extend their gratitude for the support provided by the New Technology Research Center, Tehran, Iran.

Conflict of Interest

The authors declared no potential conflicts of interest with respect to the research, authorship and publication of this article.

Funding

This study started after receiving its scientific ethical approval from Isfahan University of Medical Sciences that registered inquiry and funding under the No. 198091 and IR.MUI.RESEARCH. REC.1398.218 (clinical research section).

References

[1] Xue, P., Pauly, S., Gan, W., Jiang, S., Fan, H., Ning, Z., Sun, J. Enhanced tensile plasticity of a CuZr-based bulk metallic glass composite induced by ion irradiation. *Journal of Materials Science & Technology*, 35(10), 2019, 2221-2226.
[2] Moradi-Dastjerdi, R., Aghadavoudi, F. Static analysis of functionally graded nanocomposite sandwich plates reinforced by defected CNT. *Composite Structures*, 200, 2018, 839-848.
[3] Peng, Y., Zarringhalam, M., Barzinjy, A. A., Toghraie, D., Afrand, M. Effects of surface roughness with the spherical shape on the fluid flow of Argon atoms flowing into the microchannel, under boiling condition using molecular dynamic simulation. *Journal of Molecular Liquids*, 297, 2020, 111650.
[4] Aghadavoudi, F., Golestanian, H., Tadi Beni, Y. Investigating the effects of CNT aspect ratio and agglomeration on elastic constants of crosslinked polymer nanocomposite using multiscale modeling. *Polymer Composites*, 39(12), 2018, 4513-4523.
[5] Aghdam, H. A., Sanatizadeh, E., Motififard, M., Aghadavoudi, F., Saber-Samandari, S., Esmaeili, S., Khandan, A. Effect of calcium silicate nanoparticle on surface feature of calcium phosphates hybrid bio-nanocomposite using for bone substitute application. *Powder Technology*, 361, 2020, 917-929.
[6] Sahmani, S., Saber-Samandari, S., Shahali, M., Yekta, H. J., Aghadavoudi, F., Montazeran, A. H. Khandan, A. Mechanical and biological performance of axially loaded novel bio-nanocomposite sandwich plate-type implant coated by biological polymer thin film. *Journal of the Mechanical Behavior of Biomedical Materials*, 88, 2018 238-250.
[7] Ghasemi, M., Nejad, M. G., Bagzibagli, K. Knowledge Management Orientation: An Innovative Perspective to Hospital Management. *Iranian Journal of Public Health*, 46(12), 2017, 1639.
[8] Ghadirinejad, M., Atasoylu, E., Izbirak, G., GHA-SEMI, M. A Stochastic Model for the Ethanol Pharmacokinetics. *Iranian Journal of Public Health*, 45(9), 2016, 1170.
[9] Ghasemi, M., Aghajani, M. A., Faraji, A., & Nejad, M. S. Relationship between incidence and severity of Alternaria blight disease on different species of Brassica in Gonbad region. *Iranian Journal of Plant Path*, 49(1), 2013, 17-19.
[10] Karamian, E., Nasehi, A., Saber-Samandari, S., Khandan, A. Fabrication of hydroxyapatite-baghdadite nanocomposite scaffolds coated by PCL/Bioglass with polyurethane polymeric sponge technique. *Nanomedicine Journal*, 4(3), 2017, 177-183.
[11] Salami, M. A., Kaveian, F., Rafienia, M., Saber-Samandari, S., Khandan, A., Naeimi, M. Electrospun polycaprolactone/lignin-based nanocomposite as a novel tissue scaffold for biomedical applications. *Journal of Medical Signals and Sensors*, 7(4), 2017, 228.
[12] Montazeran, A. H., Saber Samandari, S., Khandan, A. Artificial intelligence investigation of three silicates bioceramics-magnetite bio-nanocomposite: Hyperthermia and biomedical applications. *Nanomedicine Journal*, 5(3), 2018, 163-171.
[13] Esmaeili, S., Shahali, M., Kordjamshidi, A., Torkpoor, Z., Namdari, F., Samandari, S. S., Khandan, A. An artificial blood vessel fabricated by 3D printing for pharmaceutical application. *Nanomedicine Journal*, 6(3), 2019, 183-194.
[14] Barbaz-I, R. *Experimental determining of the elastic modulus and strength of composites reinforced with two nanoparticles*, Doctoral dissertation, MSc Thesis, School of Mechanical Engineering Iran University of Science and Technology, Tehran, Iran.
[15] Moeini, M., Barbaz Isfahani, R., Saber-Samandari, S., Aghdam, M. M. Molecular dynamics simulations of the effect of temperature and strain rate on mechanical properties of graphene–epoxy nanocomposites. *Molecular Simulation*, 46(6), 2020, 476-486.
[16] Razmjooee, K., Saber-Samandari, S., Keshvari, H., Ahmadi, S. Improving anti thrombogenicity of nanofibrous polycaprolactone through surface modification. *Journal of Biomaterials Applications*, 34(3), 2019, 408-418.
[17] Murugan, R., Ramakrishna, S. Crystallographic study of hydroxyapatite bioceramics derived from various sources. *Crystal Growth & Design*, 5(1), 2005, 111-112.
[18] Uhm, S. H., Lee, S. B., Song, D. H., Kwon, J. S., Han, J. G., Kim, K. N. Fabrication of bioactive, antibacterial TiO2 nanotube surfaces, coated with magnetron sputtered Ag nanostructures for dental applications. *Journal of Nanoscience and Nanotechnology*, 14(10), 2014, 7847-7854.
[19] Eshraghi, S., Das, S. Mechanical and microstructural properties of polycaprolactone scaffolds with one-dimensional, two-dimensional, and three-dimensional orthogonally oriented porous architectures produced by selective laser sintering. *Acta Biomaterialia*, 6(7), 2010, 2467-2476.
[20] Maghsoudlou, M. A., Isfahani, R. B., Saber-Samandari, S., & Sadighi, M. Effect of interphase, curvature and agglomeration of SWCNTs on mechanical properties of polymer-based nanocomposites: Experimental and numerical investigations. *Composites Part B: Engineering*, 175, 2019, 107-119.
[21] Monshi, M., Esmaeili, S., Kolooshani, A., Moghadas, B. K., Saber-Samandari, S., & Khandan, A. A novel three-dimensional printing of electroconductive scaffolds for bone cancer therapy application. *Nanomedicine Journal*, 7(2), 2020, 138-148.
[22] Esmaeili, S., Aghdam, H. A., Motififard, M., Saber-Samandari, S., Montazeran, A. H., Bigonah, M., Khandan, A. A porous polymeric–hydroxyapatite scaffold used for femur fractures treatment: fabrication, analysis, and simulation. *European Journal of Orthopaedic Surgery & Traumatology*, 30(1), 2020, 123-131.
[23] Aghadavoudi, F., Golestanian, H., Tadi Beni, Y. Investigating the effects of resin crosslinking ratio on mechanical properties of epoxy-based nanocomposites using molecular dynamics. *Polymer Composites*, 38, 2017, E433-E442.
[24] Montazeri, A., Sadeghi, M., Naghdabadi, R., Rafii-Tabar, H. Multiscale modeling of the effect of carbon nanotube orientation on the shear deformation properties of reinforced polymer-based composites. *Physics Letters A*, 375(14), 2011, 1588-1597.
[25] Marcadon, V., Brown, D., Hervé, E., Melé, P., Albérola, N. D., Zaoui, A. Confrontation between Molecular Dynamics and micromechanical approaches to investigate particle size effects on the mechanical behaviour of polymer nanocomposites. *Computational Materials Science*, 79, 2013, 495-505.
[26] Farazin, A., Aghdam, H. A., Motififard, M., Aghadavoudi, F., Kordjamshidi, A., Saber-Samandari, S., Khandan, A. A polycaprolactone bio-nanocomposite bone substitute fabricated for femoral fracture approaches: Molecular dynamic and micro-mechanical Investigation. *Journal of Nanoanalysis*, 6(3), 2019, 172-184
[27] Saber-Samandari, S., Yekta, H., Ahmadi, S., Alamara, K. The role of titanium dioxide on the morphology, microstructure, and bioactivity of grafted cellulose/hydroxyapatite nanocomposites for a potential application in bone repair. *International Journal of Biological Macromolecules*, 106, 2018, 481-488.
[28] Saber-Samandari, S., Yekta, H., Saber-Samandari, S. Effect of iron substitution in hydroxyapatite matrix on swelling properties of composite bead. *JOM*, 9(1), 2015, 19-25.
[29] Joneidi Yekta, H., Shahali, M., Khorshidi, S., Rezaei, S., Montazeran, A. H., Samandari, S. S., Khandan, A. Mathematically and experimentally defined porous bone scaffold produced for bone substitute application. *Nanomedicine Journal*, 5(4), 2018, 227-234.

[30] Tahririan, M. A., Motififard, M., Omidian, A., Aghdam, H. A., Esmaeali, A. Relationship between bone mineral density and serum vitamin D with low energy hip and distal radius fractures: A case-control study. *Archives of Bone and Joint Surgery*, 5(1), 2017, 22.
[31] Motififard, M., Vakili, M., Moezi, M. Short-Time Influence of Totah Hip Arthroplasty on Patients with Sever Hip Ostheoarthritis. *Journal of Isfahan Medical School*, 31(237), 2013, 1-10.
[32] Sahmani, S., Shahali, M., Khandan, A., Saber-Samandari, S., Aghdam, M. M. Analytical and experimental analyses for mechanical and biological characteristics of novel nanoclay bio-nanocomposite scaffolds fabricated via space holder technique. *Applied Clay Science*, 165, 2018, 112-123.
[33] Khandan, A., Karamian, E., Bonakdarchian, M. Mechanochemical synthesis evaluation of nanocrystalline bone-derived bioceramic powder using for bone tissue engineering. *Dental Hypotheses*, 5(4), 2014, 155.
[34] Heydary, H. A., Karamian, E., Poorazizi, E., Khandan, A., Heydaripour, J. A novel nano-fiber of Iranian gum tragacanth-polyvinyl alcohol/nanoclay composite for wound healing applications. *Procedia Materials Science*, 11, 2015, 176-182.
[35] Ghayour, H., Abdellahi, M., Nejad, M. G., Khandan, A., Saber-Samandari, S. Study of the effect of the Zn 2+ content on the anisotropy and specific absorption rate of the cobalt ferrite: the application of Co 1– x Zn x Fe $_2$ O $_4$ ferrite for magnetic hyperthermia. *Journal of the Australian Ceramic Society*, 54(2), 2018, 223-230.
[36] Karamian, E., Khandan, A., Kalantar Motamedi, M. R., Mirmohammadi, H. Surface characteristics and bioactivity of a novel natural HA/zircon nanocomposite coated on dental implants. *BioMed Research International*, Article ID 410627, 2014, 10p.
[37] Razavi, M., Khandan, A. Safety, regulatory issues, long-term biotoxicity, and the processing environment. In *Nanobiomaterials Science, Development and Evaluation*, Woodhead Publishing, 2017.
[38] Karamian, E. B., Motamedi, M. R., Mirmohammadi, K., Soltani, P. A., Khandan, A. M. Correlation between crystallographic parameters and biodegradation rate of natural hydroxyapatite in physiological solutions. *Indian Journal of Scientific Research*, 4(3), 2014, 92-9.
[39] Crane, G. M., Ishaug, S. L., Mikos, A. G. Bone tissue engineering. *Nature Medicine*, 1(12), 1995, 1322-1324.
[40] Irandoust, S., Müftü, S. The interplay between bone healing and remodeling around dental implants. *Scientific Reports*, 10(1), 2020, 1-10.
[41] Darwich, A., Nazha, H., Daoud, M. Effect of Coating Materials on the Fatigue Behavior of Hip Implants: A Three-dimensional Finite Element Analysis. *Journal of Applied and Computational Mechanics*, 6(2), 2020, 284-295.
[42] Yang, W., Meyers, M. A., & Ritchie, R. O. Structural architectures with toughening mechanisms in Nature: A review of the materials science of Type-I collagenous materials. *Progress in Materials Science*, 103, 2019, 425-483.

ORCID iD

Ashkan Farazin https://orcid.org/0000-0003-4371-2799
Farshid Aghadavoudi https://orcid.org/ 0000-0002-9805-3770
Mehdi Motififard https://orcid.org/0000-0003-2597-3063
Saeed Saber-Samandari https://orcid.org/0000-0003-1975-7436
Amirsalar Khandan https://orcid.org/0000-0001-8878-5233

How to cite this article: Farazin, A., Aghadavoudi, F., Motififard, M., Saber-Samandari, S., Khandan, A. Nanostructure, Molecular Dynamics Simulation and Mechanical Performance of PCL Membranes Reinforced with Antibacterial Nanoparticles, *J. Appl. Comput. Mech.*, 7(4), 2021, 1907–1915. https://doi.org/10.22055/JACM.2020.32902.2097